Steel and Composite Structures, *Vol. 36, No. 6 (2020) 689-702*
DOI: https://doi.org/10.12989/scs.2020.36.6.689

Dynamics of graphene-nanoplatelets reinforced composite nanoplates including different boundary conditions

Behrouz Karami*[1], Davood Shahsavari[1], Ali Ordookhani[2], Parastoo Gheisari[3], Li Li[4] and Arameh Eyvazian**[5,6]

[1]*Department of Mechanical Engineering, Marvdasht Branch, Islamic Azad University, Marvdasht, Iran*
[2]*Department of Civil Engineering, School of Science and Engineering, Sharif University of Technology, International Campus, P.O. Box 79417-76655, Kish Island, Iran*
[3]*School of Mechanical Engineering, Shiraz University, Shiraz, Iran*
[4]*State Key Laboratory of Digital Manufacturing Equipment and Technology, School of Mechanical Science and Engineering, Huazhong University of Science and Technology, Wuhan 430074, China*
[5]*Institute of Research and Development, Duy Tan University, Da Nang 550000, Vietnam*
[6]*Faculty of Electrical – Electronic Engineering, Duy Tan University, Da Nang 550000, Vietnam*

(*Received March 3, 2020, Revised August 15, 2020, Accepted August 21, 2020*)

Abstract. The current study deals with the size-dependent free vibration analysis of graphene nanoplatelets (GNPs) reinforced polymer nanocomposite plates resting on Pasternak elastic foundation containing different boundary conditions. Based on a four variable refined shear deformation plate theory, which considers shear deformation effect, in conjunction with the Eringen nonlocal elasticity theory, which contains size-dependency inside nanostructures, the equations of motion are established through Hamilton's principle. Moreover, the effective material properties are estimated via the Halpin-Tsai model as well as the rule of mixture. Galerkin's mathematical formulation is utilized to solve the equations of motion for the vibrational problem with different boundary conditions. Parametrical examples demonstrate the influences of nonlocal parameter, total number of layers, weight fraction and geometry of GNPs, elastic foundation parameter, and boundary conditions on the frequency characteristic of the GNPs reinforced nanoplates in detail.

Keywords: free vibration; nanocomposites; reinforcement; Graphene nanoplatelet; boundary conditions

1. Introduction

Finding free vibration response of structures is one of the primary tasks in structural analysis so that a great deal of pioneer mechanical studies has been conducted on this issue so far (Khan *et al.* 2011, Panda and Singh 2013, Bounouara *et al.* 2016, Hebali *et al.* 2016, Mehar and Panda 2016, Dash *et al.* 2018, Houari *et al.* 2018, Farajpour *et al.* 2019, Kumar *et al.* 2019, Shahsavari *et al.* 2019). Reinforced structures, are multifunctional structures, which prepare great advances designing smart structures (Singh *et al.* 2019). These structures can be used in some devices (such as turbines, blades) because of its great properties (i.e., high strength and stiffness). In the recent decade, in order to reinforce the structures some advanced polymeric composite matrix, including Carbon Nanotubes (CNTs), Graphene, Graphene Platelets (GPLs) and GNPs are utilized for special aims. The mechanical properties of GPLs, single-walled CNTs and multi-walled CNTs reinforced epoxy nanocomposites were reported by (Rafiee *et al.* 2009) in which they showed that the strength and stiffness, which can be achieved with 1% of the weight fraction in the CNTs, can be easily achieved for GPLs with 0.1% of weight fraction. This positive point creates a great potential for using nanocomposites like GPLs and CNTs in some advanced and smart structures more than before. In this respect, some experimental, analytical, and numerical studies conducted to show the mechanical characteristics of reinforced structures made of beams, plates, and shells (Mehar and Panda 2015, Mehar and Panda 2016, Mehar *et al.* 2016, Mehar *et al.* 2017, Mehar *et al.* 2017, Mehar *et al.* 2017, Mehar *et al.* 2017, Bisen *et al.* 2018, Mehar and Kumar Panda 2018, Mehar and Panda 2018, Mehar *et al.* 2018, Dash *et al.* 2019, Eyvazian *et al.* 2019, Karami *et al.* 2019, Karami *et al.* 2019, Mehar and Panda 2019, Mehar and Panda 2019, Mehar, Panda *et al.* 2019; Mehar, Panda *et al.* 2019; Eyvazian, Shahsavari *et al.* 2020, Karami *et al.* 2020, Karami and Shahsavari 2020, Mehar *et al.* 2020, Mehar and Panda 2020, Mehar *et al.* 2020, Motezaker and Eyvazian 2020). To review some of studies on GPLs reinforced structures, the dynamics of GPLs reinforced polymeric nanocomposite plates were studied by (Song *et al.* 2017) via Navier solution-based technique. In another work (Song *et al.* 2018) studied the bending and buckling problem of mentioned structures using an analytical solution. Employing a numerical approximate based on Finite Element Method (FEM) an investigation was carried out by (Zhao *et al.* 2017) for static and dynamics of

*Corresponding author, Senior lecturer
E-mail: behrouz.karami@miau.ac.ir
**Ph.D.
E-mail: arameheyvazian@duytan.edu.vn

ISSN: 1229-9367 (Print), 1598-6233 (Online)

trapezoidal nanocomposite plates reinforced with GPLs. (Kitipornchai *et al.* 2017) investigated the free vibrations and elastic buckling of porous beams reinforced with GPLs via Timoshenko beam theory and Ritz method. Wave propagation of GNPs (GNPs) polymer composite nanoplates was investigates using a refined plate theory by (Karami *et al.* 2020). Free vibrations and stability of graphene-reinforced porous nanocomposite plates were studied by (Yang *et al.* 2018) using Chebyshev-Ritz method. Nonlinear vibration and post-buckling of porous nanocomposites reinforced with graphene were investigated by (Chen *et al.* 2017) employing Timoshenko beam theory and Ritz method. Doubly-curved shallow shells reinforced with GPLs for vibration and bending problems via a higher order shear deformation theory and Navier technique were analyzed by (Wang *et al.* 2018). Using a numerical method and a unified higher-order shear deformable plate model, the nonlinear vibration of polymer nanocomposite rectangular plates reinforced by GPLs was studied by (Gholami and Ansari 2018). As shortly reviewed, there is a shortcoming for analysis of GNPs reinforced structures when the scale of this structure tends to nanoscale.

Nowadays, with the development and growth of using miniature systems, a great deal of research has been made by many researchers on the precise understanding of materials at micro/nano scales. In order to study the size-dependent analysis of these structures, some theories including small-scale parameters were presented so that the small-scale effects can be incorporated when the scale tends to micro/nanoscales (Ghayesh *et al.* 2016, Farajpour *et al.* 2018, Ghayesh 2018, Farajpour *et al.* 2019, Ghayesh and Farajpour 2019, Karami *et al.* 2020). As one of these well-known size-dependent theories, the nonlocal elasticity theory presented by Eringen has been employed by many researchers to investigate the stiffness-softening mechanism of various nanostructures (Ghayesh 2014, Quaresimin *et al.* 2016, Bouafia *et al.* 2017, Shahsavari *et al.* 2017, Karami *et al.* 2018, Mehar *et al.* 2018, Benahmed *et al.* 2019, Farajpour *et al.* 2019, Fattahi *et al.* 2019, Karami *et al.* 2019, Shahsavari *et al.* 2019, Shahsavari *et al.* 2019, Tahouneh *et al.* 2019, Gholipour and Ghayesh 2020, Karami and Janghorban 2020). In the recent years, size-dependent analysis on nanostructure systems reinforced with CNTs and GNPs have been conducted in some studies. (Phung-Van *et al.* 2017) investigated the size-dependent static and dynamics of composite nanoplates reinforced with CNTs based on the isogeometric analysis. (Sahmani *et al.* 2018) studied the nonlinear static of GNPs reinforced porous beams using Galerkin's method. Size-dependent vibrations responses of GNPs reinforced polymeric composite nanoplates were analyzed by (Arefi *et al.* 2018). (Thanh *et al.* 2018) studied the size-dependent isogeometric static and vibration analysis of composite nanoplates reinforced with CNTs using a higher order shear deformation theory. (Farzam and Hassani 2018) investigated the size-dependent thermal and mechanical buckling response of composite plate reinforced with CNTs via isogeometric approach. More recently, (Karami *et al.* 2018) studied the size-dependent stability, bending and vibration problems of composite plates reinforced with CNTs using the second-order shear deformation plate theory and Navier solution-based technique. However, considering boundary conditions in combination with size-dependent effect has some important gaps.

The boundary condition is one of the main issues that need to be considered in different mechanical analyzes of both size-dependent and size independent structures. Because the results of static and dynamic analyses are highly dependent on boundary conditions, which this issue has been devised for different structures (Canales and Mantari 2018, Imran *et al.* 2018). Typically, mechanics of simply supported boundary conditions investigate, but it is universally accepted that overall boundary condition can be a combination of simply supported, free, or clamped boundary conditions. To cite related articles, (Zhong *et al.* 2018) studied the vibrational response of composite rectangular plates reinforced with CNTs under the impacts of arbitrary boundary conditions using an enhanced Ritz method. Composite plates were analyzed by (Imran *et al.* 2018) for effects of delamination size, stacking sequence and boundary conditions on the vibration response using FEM. Free vibrations of thick porous rectangular plates with different boundary conditions were studied by (Zhao *et al.* 2018) via the three-dimensional exact solution and the Rayleigh-Ritz process. (Canales and Mantari 2018) investigated the various boundary conditions effects on the dynamics of isotropic laminated beams via unified formulation and Ritz method. Jacobi-Ritz method was utilized to investigate the vibrations response of cracked laminated composite beams by (Kim *et al.* 2018) for different boundary conditions. The electro-thermo-mechanical vibration behavior FG piezoelectric plate was studied by (Barati and Zenkour 2018). In their work, the effect of different boundary conditions was also investigated via an analytical approach. Size-dependent vibration and stability responses of graphene sheets including different boundary conditions were analyzed by (Radić and Jeremić 2017) using Galerkin's method. They showed that this method is in good agreement with exact results for size-dependent analysis of structures with different boundary conditions using determined shape functions.

Hence, performing an analysis on the size-dependent vibrational behavior of GNPs-reinforced FG-PC nanoplates with the use of a higher-order refined plate theory and Eringen nonlocal differential model using Galerkin's method is the main aim of this study. Further, inside the polymer matrix, four different patterns of reinforcement distributions are supposed. The Halpin-Tsai model and a rule of mixture are utilized to estimate the properties of the material with GNPS distributed in the thickness direction of the plate. The governing equations and boundary conditions are derived via Hamilton's principle and solved using Galerkin's method for vibrational problem including different boundary conditions. Also, the effects of some important parameters such as the geometry of GNPs, the total number of layers, the weight fraction of GNPs, Winkler-Pasternak foundation coefficients, nonlocal parameter, and boundary conditions on the free vibrations of GNPs reinforce FG-PC nanoplates are studied. It is

hoped that the present numerical results can serve as a benchmark for future investigation of GNPs reinforced nanoplates.

2. Eringen nonlocal differential model

(Eringen 1983) presented a non-classical model of continuum mechanics in which the size-dependent effects are considered by only one small-scale parameter. In this model, "the stress field at a reference point x in an elastic continuum media depends not only on the strain at that point but also on strains at all other points in the domain". So, the stress tensor is given by

$$\tau_{ij} = \int_V \alpha(|x'-x|,\tau)\sigma_{ij}(x')dV' \tag{1}$$

where σ_{ij} and τ_{ij} are, respectively, the local and nonlocal stress tensors. $\alpha(|x'-x|,\tau)$ refers to the nonlocal kernel. $\tau=e_0a/\ell$ refers to a small-scale factor where e_0 is determined experimentally, "ℓ is the external characteristic length (e.g., lattice parameter) and a is an external characteristic length (e.g., crack length, wavelength) of the material".

For the sake of simplification, to consider the scale effects, the following differential constitutive relation consequent (but not equivalent) to Eq. (1) is used.

$$\left[1-(e_0a)^2\nabla^2\right]\sigma_{ij} = C_{ijkl}\varepsilon_{kl} \tag{2}$$

where ∇^2 is the Laplacian operator in Cartesian coordinate, and C_{ijkl} denote elastic matrix components.

3. Basic formulation

3.1 Material properties of composite nanoplate reinforced with GNPs

Consider a plate made of polymeric nanocomposites with the length a, width b, and thickness h which is composed N_L layers with the thickness $\delta h=h/N_L$ (see Fig. 1). GNPs are utilized as the filler inside each layer or the reinforcement phase.

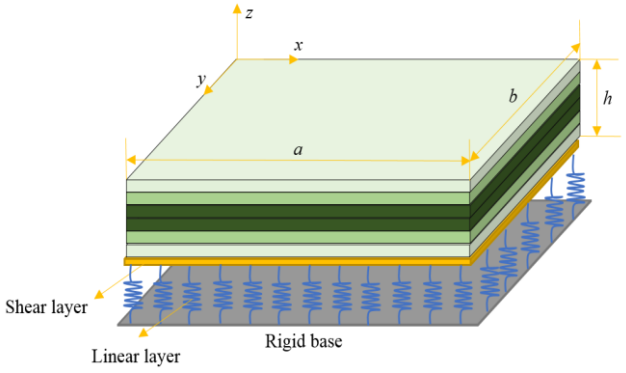

Fig. 1 The geometry of GNPs reinforce nanocomposite plate

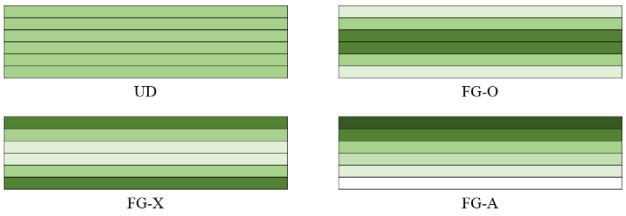

Fig. 2 Patterns of GNPs distributions.

The reinforcement of GNPs is dispersed in a polymer material via four different patterns, as shown in Fig. 2. Uniform and three non-uniform distributions patterns of GNPs are considered.

The density of GNPs and a polymer matrix are defined by ρ_{GNP} and ρ_M, respectively. ν_M and ν_{GNP} are, respectively, the Poisson's ratio of a polymer matrix and GNPs. Using the role of mixture, the effective density and Poisson's ratio for the GNPs reinforced nanocomposite plate for the k-layer is expressed as

$$\rho_c^{(k)} = \rho_{GNP}V_{GNP}^{(k)} + \rho_M V_M^{(k)} \tag{3}$$

$$\nu_c^{(k)} = \nu_{GNP}V_{GNP}^{(k)} + \nu_M V_M^{(k)} \tag{4}$$

in which $V_{GNP}^{(k)}$ denotes the volume fraction of GNPs, defined as

$$V_{GNP}^{(k)} = \frac{g_{GNP}^{(k)}}{g_{GNP}^{(k)} + \frac{\rho_{GNP}}{\rho_M}(1-g_{GNP}^{(k)})} \tag{5}$$

herein $g_{GNP}^{(k)}$ indicates the weight fraction for the k-layer of GNPs. Fig. 2 shows different GNPs distributions, and the weight fraction of GNPs is expressed as follows (Song *et al.* 2018)

$$g_{GNP}^{(k)} = \begin{cases} g_{GNP}^{*} & \text{UD} \\ \dfrac{4g_{GNP}^{*}\left(\frac{N_L+1}{2} - \left|k - \frac{N_L+1}{2}\right|\right)}{(2+N_L)} & \text{FG-O} \\ \dfrac{4g_{GNP}^{*}\left(\frac{1}{2} + \left|k - \frac{N_L+1}{2}\right|\right)}{(2+N_L)} & \text{FG-X} \\ 2kg_{GNP}^{*}/(N_L+1) & \text{FG-A} \end{cases} \tag{6}$$

with g_{GNP}^{*} being the weight fraction of GNPs. The effective Young's moduli are estimated through the Halpin-Tsai model and given by (Yang *et al.* 2018)

$$E_{eff}^{(k)} = \frac{3}{8}\frac{1+\xi_L\eta_L V_{GNP}^{(k)}}{1-\eta_L V_{GNP}^{(k)}}\times E_M + \frac{5}{8}\frac{1+\xi_T\eta_T V_{GNP}^{(k)}}{1-\eta_T V_{GNP}^{(k)}}\times E_M \tag{7}$$

in which Young's modulus of a polymer matrix is indicated by E_M. The subscripts 'L' and 'T' account for the longitudinal and transverse effects, respectively. To account for the effect of Young's modulus of GNPs and the

geometry of GNPs, four additional parameters (η_L, η_T) and (ξ_L, ξ_T) are defined as follows

$$\eta_L = \frac{\frac{E_{GNP}}{E_M}-1}{\frac{E_{GNP}}{E_M}+\xi_L}, \eta_T = \frac{\frac{E_{GNP}}{E_M}-1}{\frac{E_{GNP}}{E_M}+\xi_W} \tag{8}$$

$$\xi_L = 2\frac{l_{GNP}}{h_{GNP}}, \xi_T = 2\frac{w_{GNP}}{h_{GNP}} \tag{9}$$

where l_{GNP}, w_{GNP}, and h_{GNP} are, respectively, the average length, width, and thickness of the GNPs. Notice that Young's modulus of GNPs is indicated by E_{GNP}.

3.2 Kinematic relations

The equations of motion are obtained based on the following displacement fields (Zidi *et al*. 2014)

$$\begin{aligned} u(x,y,z,t) &= u_0(x,y,t) - z\frac{\partial w_b}{\partial x} - f(z)\frac{\partial w_s}{\partial x} \\ v(x,y,z,t) &= v_0(x,y,t) - z\frac{\partial w_b}{\partial y} - f(z)\frac{\partial w_s}{\partial y} \\ w(x,y,z,t) &= w_b(x,y,t) + w_s(x,y,t) \end{aligned} \tag{10}$$

where u_0 and v_0 indicate the displacements along the x and y directions, respectively; the bending and shear components of the transverse displacement respectively shows by w_b and w_s; $f(z)$is the shape functions and presented as follows

$$f(z) = -\frac{z}{4} + \frac{5}{3}z\left(\frac{z}{h}\right)^2 \tag{11}$$

The stress-strain relation of a k-layer polymer composite nanoplate can be expressed as

$$(1-\mu^2\nabla^2)\begin{bmatrix}\sigma_x\\ \sigma_y\\ \tau_{yz}\\ \tau_{xz}\\ \tau_{xy}\end{bmatrix} = \begin{bmatrix} C_{11}^{(k)} & C_{12}^{(k)} & 0 & 0 & 0 \\ C_{12}^{(k)} & C_{22}^{(k)} & 0 & 0 & 0 \\ 0 & 0 & C_{44}^{(k)} & 0 & 0 \\ 0 & 0 & 0 & C_{55}^{(k)} & 0 \\ 0 & 0 & 0 & 0 & C_{66}^{(k)} \end{bmatrix}\begin{bmatrix}\varepsilon_x\\ \varepsilon_y\\ \gamma_{yz}\\ \gamma_{xz}\\ \gamma_{xy}\end{bmatrix} \tag{12}$$

where

$$\begin{aligned} C_{11}^{(k)} &= C_{22}^{(k)} = \frac{E_c^{(k)}}{1-(\nu_c^{(k)})^2} \\ C_{12}^{(k)} &= C_{21}^{(k)} = \nu_c^{(k)} C_{11}^{(k)} \\ C_{44}^{(k)} &= C_{55}^{(k)} = C_{66}^{(k)} = \frac{E_c^{(k)}}{2(1+\nu_c^{(k)})} \end{aligned} \tag{13}$$

in which $\mu=e_0a$. Non-zero strain-displacement relations are expressed as the following formulas

$$\begin{aligned} \begin{Bmatrix}\varepsilon_x\\ \varepsilon_y\\ \gamma_{xy}\end{Bmatrix} &= \begin{Bmatrix}\varepsilon_x^0\\ \varepsilon_y^0\\ \gamma_{xy}^0\end{Bmatrix} + z\begin{Bmatrix}k_x^b\\ k_y^b\\ k_{xy}^b\end{Bmatrix} + f(z)\begin{Bmatrix}k_x^s\\ k_y^s\\ k_{xy}^s\end{Bmatrix} \\ \begin{Bmatrix}\gamma_{yz}\\ \gamma_{xz}\end{Bmatrix} &= g\begin{Bmatrix}\gamma_{yz}^0\\ \gamma_{xz}^0\end{Bmatrix},\ g = 1-\frac{\partial f}{\partial z} \end{aligned} \tag{14}$$

in which

$$\begin{aligned} &\begin{Bmatrix}\varepsilon_x\\ \varepsilon_y\\ \gamma_{xy}\end{Bmatrix} = \begin{Bmatrix}\frac{\partial u_0}{\partial x}\\ \frac{\partial v_0}{\partial y}\\ \frac{\partial u_0}{\partial y}+\frac{\partial v_0}{\partial x}\end{Bmatrix}, \begin{Bmatrix}k_x^b\\ k_y^b\\ k_{xy}^b\end{Bmatrix} = \begin{Bmatrix}-\frac{\partial^2 w_b}{\partial x^2}\\ -\frac{\partial^2 w_b}{\partial y^2}\\ -2\frac{\partial^2 w_b}{\partial x\,\partial y}\end{Bmatrix} \\ &\begin{Bmatrix}k_x^s\\ k_y^s\\ k_{xy}^s\end{Bmatrix} = \begin{Bmatrix}-\frac{\partial^2 w_s}{\partial x^2}\\ -\frac{\partial^2 w_s}{\partial y^2}\\ -2\frac{\partial^2 w_s}{\partial x\,\partial y}\end{Bmatrix}, \begin{Bmatrix}\gamma_{yz}^0\\ \gamma_{xz}^0\end{Bmatrix} = \begin{Bmatrix}\frac{\partial w_s}{\partial y}\\ \frac{\partial w_s}{\partial x}\end{Bmatrix} \end{aligned} \tag{15}$$

Using Hamilton's principle, Euler-Lagrange equations can be derived as

$$\int_0^t \delta(U-K+V)dt = 0 \tag{16}$$

where $\delta U, \delta K$ and δV refer to the variation of strain energy, kinetic energy, and work done by applied forces, respectively. The variation of strain energy is expressed as

$$\begin{aligned} \delta U &= \int_{-h/2}^{h/2}\int_A \left[\sigma_{ij}\delta\varepsilon_{ij}\right]dAdz \\ &= \int_A \Big[N_x\delta\varepsilon_x^0 + N_y\delta\varepsilon_y^0 + N_{xy}\delta\gamma_{xy}^0 + M_x^b\delta k_x^b + M_y^b\delta k_y^b \\ &+ M_{xy}^b\delta k_{xy}^b + M_x^s\delta k_x^s + M_y^s\delta k_y^s + M_{xy}^s\delta k_{xy}^s + Q_{yz}^s\gamma_{yz}^0 \\ &+ Q_{xz}^s\gamma_{xz}^0\Big]dA = 0 \end{aligned} \tag{17}$$

where

$$\begin{Bmatrix} N_x & N_y & N_z \\ M_x^b & M_y^b & M_{xy}^b \\ M_x^s & M_y^s & M_{xy}^s \end{Bmatrix} = \int_{-h/2}^{h/2}(\sigma_x,\sigma_y,\tau_{xy})\begin{Bmatrix}1\\ z\\ f\end{Bmatrix}dz \tag{18}$$

and

$$(Q_{xz}^s, Q_{yz}^s) = \int_{-h/2}^{h/2} g(\tau_{xz},\tau_{yz})dz \tag{19}$$

The first variation of work done can be expressed as

$$\delta V = \int_{-h/2}^{h/2}\int_A \left[k_P\left(\frac{\partial}{\partial x}\frac{\partial\delta w}{\partial x} + \frac{\partial}{\partial y}\frac{\partial\delta w}{\partial y}\right) - k_W\delta w\right]dAdz \tag{20}$$

where k_W and k_P are elastic foundation parameters. The kinetic energy variations can be given as

$$\begin{aligned} \delta K &= \int_{-h/2}^{h/2}\int_A \left[\dot{u}_0\delta\dot{u}_0 + \dot{v}_0\delta\dot{v}_0 + \dot{w}\,\delta\dot{w}\right]dAdz \\ &= \int_A \Big\{I_0\left(\dot{u}_0\delta\dot{u}_0 + \dot{v}_0\delta\dot{v}_0 + (\dot{w}_b+\dot{w}_s)(\delta\dot{w}_b+\delta\dot{w}_s)\right) \\ &- I_1\left(\dot{u}_0\frac{\partial\delta\dot{w}_b}{\partial x} + \frac{\partial\dot{w}_b}{\partial x}\delta\dot{u}_0 + \dot{v}_0\frac{\partial\delta\dot{w}_s}{\partial y} + \frac{\partial\dot{w}_s}{\partial y}\delta\dot{v}_0\right) \\ &- J_1\left(\dot{u}_0\frac{\partial\delta\dot{w}_s}{\partial x} + \frac{\partial\dot{w}_s}{\partial x}\delta\dot{u}_0 + \dot{v}_0\frac{\partial\delta\dot{w}_s}{\partial y} + \frac{\partial\dot{w}_s}{\partial y}\delta\dot{v}_0\right) \\ &+ I_2\left(\frac{\partial\delta\dot{w}_b}{\partial x}\frac{\partial\delta\dot{w}_b}{\partial x} + \frac{\partial\delta\dot{w}_b}{\partial y}\frac{\partial\delta\dot{w}_b}{\partial y}\right) \\ &+ K_2\left(\frac{\partial\delta\dot{w}_s}{\partial x}\frac{\partial\delta\dot{w}_s}{\partial x} + \frac{\partial\delta\dot{w}_s}{\partial y}\frac{\partial\delta\dot{w}_s}{\partial y}\right) \\ &+ J_2\left(\frac{\partial\dot{w}_b}{\partial x}\frac{\partial\delta\dot{w}_s}{\partial x} + \frac{\partial\dot{w}_s}{\partial x}\frac{\partial\delta\dot{w}_b}{\partial x} + \frac{\partial\dot{w}_b}{\partial y}\frac{\partial\delta\dot{w}_s}{\partial y} + \frac{\partial\dot{w}_s}{\partial y}\frac{\partial\delta\dot{w}_b}{\partial y}\right)\Big\}dA \end{aligned} \tag{21}$$

where

$$\{I_0, I_1, J_1, I_2, J_2, K_2\} = \sum_{k=1}^{N_L} \int_{z(k)}^{z(k+z)} \{1, z, f, z^2, zf, f^2\} \rho_c^{(k)} dz \tag{22}$$

The nonlocal differential equations of motion are obtained by inserting Eqs. (17), (20) and (21) into Eq. (16) as follows

$$\delta u_0 : \frac{\partial N_x}{\partial x} + \frac{\partial N_{xy}}{\partial y} = I_0 \ddot{u}_0 - I_1 \frac{\partial \ddot{w}_b}{\partial x} - J_1 \frac{\partial \ddot{w}_s}{\partial x} \tag{23}$$

$$\delta v_0 : \frac{\partial N_{xy}}{\partial x} + \frac{\partial N_y}{\partial y} = I_0 \ddot{v}_0 - I_1 \frac{\partial \ddot{w}_b}{\partial y} - J_1 \frac{\partial \ddot{w}_s}{\partial y} \tag{24}$$

$$\begin{aligned} &\delta w_b : \frac{\partial^2 M_x^b}{\partial x^2} + 2\frac{\partial^2 M_{xy}^b}{\partial x \partial y} + \frac{\partial^2 M_y^b}{\partial y^2} - k_W w + k_P \nabla^2 w \\ &= I_0 \ddot{w} + I_1 \left(\frac{\partial \ddot{u}_0}{\partial x} + \frac{\partial \ddot{v}_0}{\partial y} \right) - I_2 \nabla^2 \ddot{w}_b - J_2 \nabla^2 \ddot{w}_s \end{aligned} \tag{25}$$

$$\begin{aligned} &\delta w_s : \frac{\partial^2 M_x^s}{\partial x^2} + 2\frac{\partial^2 M_{xy}^s}{\partial x \partial y} + \frac{\partial^2 M_y^s}{\partial y^2} + \frac{\partial Q_{xz}^s}{\partial x} + \frac{\partial Q_{yz}^s}{\partial y} - k_W w \\ &+ k_P \nabla^2 w = I_0 \ddot{w} + J_1 \left(\frac{\partial \ddot{u}_0}{\partial x} + \frac{\partial \ddot{v}_0}{\partial y} \right) - J_2 \nabla^2 \ddot{w}_b - K_2 \nabla^2 \ddot{w}_s \end{aligned} \tag{26}$$

Due to the stress-strain relations (Eq. (14)) and equations of motion (Eqs. (23-26)), the stress resultants are obtained as

$$\begin{aligned} \begin{Bmatrix} N \\ M^b \\ M^s \end{Bmatrix} &= \begin{bmatrix} A_{11} & A_{12} & 0 \\ A_{11} & A_{12} & 0 \\ 0 & 0 & A_{66} \end{bmatrix} \begin{Bmatrix} \frac{\partial u}{\partial x} \\ \frac{\partial v}{\partial y} \\ \frac{\partial u}{\partial y} + \frac{\partial v}{\partial x} \end{Bmatrix} \\ &+ \begin{bmatrix} B_{11} & B_{12} & 0 \\ B_{11} & B_{12} & 0 \\ 0 & 0 & B_{66} \end{bmatrix} \begin{Bmatrix} -\frac{\partial^2 w_b}{\partial x^2} \\ \frac{\partial^2 w_b}{\partial y^2} \\ -2\frac{\partial^2 w_b}{\partial x \partial y} \end{Bmatrix} + \begin{bmatrix} B_{11}^s & B_{12}^s & 0 \\ B_{11}^s & B_{12}^s & 0 \\ 0 & 0 & B_{66}^s \end{bmatrix} \begin{Bmatrix} -\frac{\partial^2 w_s}{\partial x^2} \\ \frac{\partial^2 w_s}{\partial y^2} \\ -2\frac{\partial^2 w_s}{\partial x \partial y} \end{Bmatrix} \end{aligned} \tag{27}$$

$$\begin{aligned} \begin{Bmatrix} M_x^b \\ M_y^b \\ M_{xy}^b \end{Bmatrix} &= \begin{bmatrix} B_{11} & B_{12} & 0 \\ B_{11} & B_{12} & 0 \\ 0 & 0 & B_{66} \end{bmatrix} \begin{Bmatrix} \frac{\partial u}{\partial x} \\ \frac{\partial v}{\partial y} \\ \frac{\partial u}{\partial y} + \frac{\partial v}{\partial x} \end{Bmatrix} \\ &+ \begin{bmatrix} D_{11} & D_{12} & 0 \\ D_{11} & D_{12} & 0 \\ 0 & 0 & D_{66} \end{bmatrix} \begin{Bmatrix} -\frac{\partial^2 w_b}{\partial x^2} \\ \frac{\partial^2 w_b}{\partial y^2} \\ -2\frac{\partial^2 w_b}{\partial x \partial y} \end{Bmatrix} + \begin{bmatrix} D_{11}^s & D_{12}^s & 0 \\ D_{11}^s & D_{12}^s & 0 \\ 0 & 0 & D_{66}^s \end{bmatrix} \begin{Bmatrix} -\frac{\partial^2 w_s}{\partial x^2} \\ \frac{\partial^2 w_s}{\partial y^2} \\ -2\frac{\partial^2 w_s}{\partial x \partial y} \end{Bmatrix} \end{aligned} \tag{28}$$

$$\begin{aligned} \begin{Bmatrix} M_x^s \\ M_y^s \\ M_{xy}^s \end{Bmatrix} &= \begin{bmatrix} B_{11}^s & B_{12}^s & 0 \\ B_{11}^s & B_{12}^s & 0 \\ 0 & 0 & B_{66}^s \end{bmatrix} \begin{Bmatrix} \frac{\partial u}{\partial x} \\ \frac{\partial v}{\partial y} \\ \frac{\partial u}{\partial y} + \frac{\partial v}{\partial x} \end{Bmatrix} \\ &+ \begin{bmatrix} D_{11}^s & D_{12}^s & 0 \\ D_{11}^s & D_{12}^s & 0 \\ 0 & 0 & D_{66}^s \end{bmatrix} \begin{Bmatrix} -\frac{\partial^2 w_b}{\partial x^2} \\ \frac{\partial^2 w_b}{\partial y^2} \\ -2\frac{\partial^2 w_b}{\partial x \partial y} \end{Bmatrix} + \begin{bmatrix} H_{11}^s & H_{12}^s & 0 \\ H_{11}^s & H_{12}^s & 0 \\ 0 & 0 & H_{66}^s \end{bmatrix} \begin{Bmatrix} -\frac{\partial^2 w_s}{\partial x^2} \\ \frac{\partial^2 w_s}{\partial y^2} \\ -2\frac{\partial^2 w_s}{\partial x \partial y} \end{Bmatrix} \end{aligned} \tag{29}$$

$$\begin{Bmatrix} Q_{xz} \\ Q_{yz} \end{Bmatrix} = \begin{bmatrix} A_{44}^s & 0 \\ 0 & A_{55}^s \end{bmatrix} \begin{Bmatrix} \frac{\partial w_s}{\partial x} \\ \frac{\partial w_s}{\partial y} \end{Bmatrix} \tag{30}$$

where

$$(A_{ij}, B_{ij}, B_{ij}^s, D_{ij}, D_{ij}^s, H_{ij}^s) = \sum_{k=1}^{N_L} \int_{z(k)}^{z(k+z)} C_{ij}^{(k)} (1, z, f, z^2, zf, f^2) dz, \ (i, j) = 1, 2, 6 \tag{31}$$

and

$$A_{44}^s = A_{55}^s = \sum_{k=1}^{N_L} \int_{z(k)}^{z(k+z)} C_{55}^{(k)} g^2 dz \tag{32}$$

According to the Eringen nonlocal differential model and applying Eqs. (27)-(30) into Eqs. (23)-(26), the nonlocal equations of motion can be expressed in terms of displacements as follow

$$\begin{aligned} &A_{11} d_{11} u_0 + A_{66} d_{22} u_0 + (A_{12} + A_{66}) d_{12} v_0 - B_{11} d_{111} w_b \\ &-(B_{12} + 2B_{66}) d_{122} w_b - B_{11}^s d_{111} w_s - (B_{12}^s + 2B_{66}^s) d_{122} w_s \\ &= \mathrm{L}_\mu (I_0 \ddot{u}_0 - I_1 d_1 \ddot{w}_b - J_1 d_1 \ddot{w}_s) = 0 \end{aligned} \tag{33}$$

$$\begin{aligned} &A_{22} d_{22} v_0 + A_{66} d_{11} v_0 + (A_{12} + A_{66}) d_{12} u_0 - B_{22} d_{222} w_b \\ &-(B_{12} + 2B_{66}) d_{112} w_b - B_{22}^s d_{222} w_s - (B_{12}^s + 2B_{66}^s) d_{112} w_s \\ &= \mathrm{L}_\mu (I_0 \ddot{v}_0 - I_1 d_2 \ddot{w}_b - J_1 d_2 \ddot{w}_s) = 0 \end{aligned} \tag{34}$$

$$\begin{aligned} &B_{11} d_{111} u_0 + (B_{12} + 2B_{66}) d_{122} u_0 + (B_{12} + 2B_{66}) d_{122} v_0 \\ &+B_{22} d_{222} v_0 - D_{11} d_{1111} w_b - 2(D_{12} + 2D_{66}) d_{1122} w_b \\ &-D_{22} d_{2222} w_b - D_{11}^s d_{1111} w_s - 2(D_{12}^s + 2D_{66}^s) d_{1122} w_s \\ &-D_{22}^s d_{2222} w_s + \mathrm{L}_\mu (-k_W w + k_P (d_{11} w + d_{22} w)) \\ &= \mathrm{L}_\mu (I_0 (\ddot{w}_b + \ddot{w}_s) + I_1 (d_1 \ddot{u}_0 + d_2 \ddot{v}_0) \\ &-I_2 (d_{11} \ddot{w}_b + d_{22} \ddot{w}_b) - J_2 (d_{11} \ddot{w}_s + d_{22} \ddot{w}_s)) = 0 \end{aligned} \tag{35}$$

$$\begin{aligned} &B_{11}^s d_{111} u_0 + (B_{12}^s + 2B_{66}^s) d_{122} u_0 + (B_{12}^s + 2B_{66}^s) d_{122} v_0 \\ &+B_{22}^s d_{222} v_0 - D_1^s d_{1111} w_b - 2(D_{12}^s + 2D_{66}^s) d_{1122} w_b \\ &-D_{22}^s d_{2222} w_b - H_{11}^s d_{1111} w_s - 2(H_{12}^s + 2H_{66}^s) d_{1122} w_s \\ &-H_{22}^s d_{2222} w_s + A_{44}^s d_{11} w_s + A_{55}^s d_{22} w_s \\ &+\mathrm{L}_\mu (-k_W w + k_P (d_{11} w + d_{22} w)) = \mathrm{L}_\mu (I_0 (\ddot{w}_b + \ddot{w}_s) \\ &+J_1 (d_1 \ddot{u}_0 + d_2 \ddot{v}_0)) + \mathrm{L}_\mu (-J_2 (d_{11} \ddot{w}_b + d_{22} \ddot{w}_b) \\ &-K_2 (d_{11} \ddot{w}_s + d_{22} \ddot{w}_s)) \end{aligned} \tag{36}$$

in which d_j, dij, d_{ijl} and d_{ijlm} are the following differential operators

$$d_i = \frac{\partial}{\partial x_i}, d_{ij} = \frac{\partial^2}{\partial x_i \partial x_j}, d_{ijl} = \frac{\partial^3}{\partial x_i \partial x_j \partial x_l}$$
$$d_{ijlm} = \frac{\partial^4}{\partial x_i \partial x_j \partial x_l \partial x_m} \quad (i, j, l, m = 1, 2) \tag{37}$$

and $L_\mu = 1 - \mu^2 (d_{11} + d_{22})$.

4. Solution procedure

Here an analytic technique is utilized for vibration problem of the nanoplate with simply-supported (S), clamped (C) or free (F) edges. These boundary conditions are introduced as follow (Sobhy 2013, Meziane *et al.* 2014, Abdelaziz, Meziane *et al.* 2017):

• Simply-supported (S)

$$w_b = w_s = Nx = Mx = 0 \text{ at } x = 0, a$$
$$w_b = w_s = Ny = My = 0 \text{ at y} = 0, \text{ b} \tag{38}$$

• Clamped (C)

$$u = v = w_b = w_s = 0 \text{ t } x = 0, a \text{ and } y = 0, b \tag{39}$$

• Free (F)

$$Mx = Mxy = Q_{xz} = 0 \text{ at } x = 0, a$$
$$My = Mxy = Q_{yz} = 0 \text{ at y} = 0, \text{ b} \tag{40}$$

The following series are suggested to satisfy the above boundary conditions.

$$u = \sum_{m=1}^{\infty} \sum_{n=1}^{\infty} U_{mn} \frac{\partial X_m(x)}{\partial x} Y_n(y) e^{i\omega t} \tag{41}$$

$$v = \sum_{m=1}^{\infty} \sum_{n=1}^{\infty} V_{mn} X_m(x) \frac{\partial Y_n(y)}{\partial y} e^{i\omega t} \tag{42}$$

$$w_b = \sum_{m=1}^{\infty} \sum_{n=1}^{\infty} W_{b\,mn} X_m(x) Y_n(y) e^{i\omega t} \tag{43}$$

$$w_s = \sum_{m=1}^{\infty} \sum_{n=1}^{\infty} W_{s\,mn} X_m(x) Y_n(y) e^{i\omega t} \tag{44}$$

herein (U_{mn}, V_{mn}, W_{bmn}, W_{smn}) denote the unknown variables and the functions X_m, Y_n according to different types of boundary conditions, which are defined in Table 1 ($\alpha = m\pi/a$, $\beta = n\pi/b$).

Inserting the above series (Eqs. (41)-(44)) in the governing equations (Eqs. (33)-(36)) leads to the following relation

$$\left([K] - [M] \omega_{mn}^2 \right) \Delta = 0 \tag{45}$$

in which $\Delta = \{U_{mn}, V_{mn}, W_{bmn}, W_{smn}\}^T$; K_{ij} and M_{ij} indicate, respectively, the stiffness and mass matrices. The natural frequencies ω_{mn} are obtained by finding the determinant of the coefficient matrix of the Eq. (45) and setting this multinomial to zero.

5. Numerical results

The presented investigation shows the impact of boundary conditions on the vibrational behavior of Functionally Graded Polymer Composite (FG-PC) macro/nano-plates reinforced with GPLs or GNPs when size effects is included. Here, the influence of Winkler-Pasternak foundation is also studied. Parametrically, the effects of the distribution patterns, weight fraction, geometries of GPLs, and total number of layers on the vibration characteristics of the FG-PC macro/nano-plates reinforced with GNPs are investigated in tabular and graphical forms. With the lack of a comprehensive study on the impact of boundary conditions for vibration behavior of the mentioned structure, it is hopeful that the results of the present study can serve as a benchmark for future works.

5.1 Validation

First of all, the accuracy of the presented mathematical model to study the nanocomposite materials reinforced with GNPs must be checked by comparing the results for free vibrations of plates with those reported by (Song *et al.* 2017) and (Arefi *et al*. 2018) and then the results are tabulated in Table 2. Further, the uniform and non-uniform reinforcement distribution patterns are also verified. At first glance, a good agreement between the different methods for several vibration modes and reinforcement patterns is observable easily.

As clarified, the impacts of different boundary conditions and nonlocality behavior on the vibrational response of the nanoplates reinforced with GNPs are main aim of this article and should be tested firstly. Hence, the results are compared with those of (Natarajan *et al.* 2012) for size-dependent free vibrations of SUS304/Si3N4 FG plate considering the effect of nonlocal parameter and boundary conditions (here simply supported and fully clamped) in Table 3. The results confirm that the presented mathematical approach can predict the size-dependent behavior of nanostructure systems including different boundary conditions effects.

As the final step of verification process, the influences of elastic foundation on the mechanical characteristics of the structure are examined for non-dimensional natural frequencies of Al/Al2O3 plate with make a comparison with the results of (Baferani *et al.* 2011) and (Shahsavari *et al.* 2018) (see Table 4). Once again, a good deal of agreement can be seen between the proposed models.

5.2 Free vibrations of FG-PC nanoplates reinforced with GNP

In this subsection, the free vibration of FG-PC nanoplates reinforced with GNPs is studied. For material properties an epoxy-matrix with Young's modulus E_M=3 GPa, Poisson's ratio ν_M=0.34, and density ρ_M=1200 kg/m^3 is considered. For reinforcements, the GNPs are utilized with Young modulus E_{GNP}=1.01 TPa, Poisson's ratio ν_{GNP}=0.186, and density ρ_{GNP}=1060 kg/m^3. The thickness of composite nanoplate is fixed at h=20 nm, and in-plane geometry is

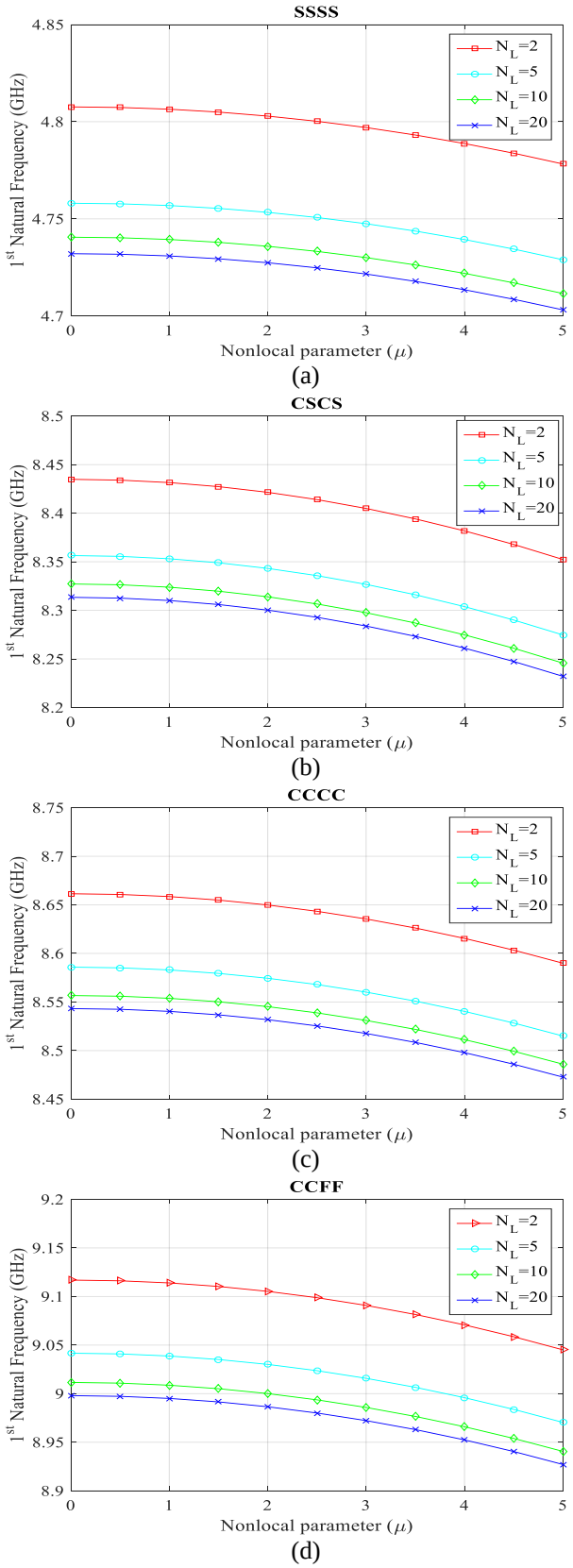

Fig. 3 1st natural frequency of the nanoplate (in GHz) vs the total number of layers (N_L) for FG-O pattern with respect to nonlocal parameters

chosen as a=b=10h and is made of GNPs with length l_{GNP}=3 nm, thickness h_{GNP}=0.7 nm, width w_{GNP}=1.8 nm (Rafiee *et al*. 2009).

Table 1 The admissible functions X_m (x) and Y_n (y) (Sobhy 2013, Meziane *et al*. 2014, Abdelaziz *et al.* 2017)

	Boundary conditions		The functions X_m and Y_n	
	At x=0, a	At y=0, b	X_m (x)	Y_n (y)
SSSS	$X_m(0)=X''_m(0)=0$	$Y_n(0)=Y''_n(0)=0$	$\sin(\alpha x)$	$\sin(\beta y)$
	$X_m(a)=X''_m(a)=0$	$Y_n(b)=Y''_n(b)=0$		
CSCS	$X_m(0)=X'_m(0)=0$	$Y_n(0)=Y'_n(0)=0$	$\sin(\alpha x)[\cos(\alpha x)-1]$	$\sin(\beta y)[\cos(\beta y)-1]$
	$X_m(a)=X''_m(a)=0$	$Y_n(b)=Y''_n(b)=0$		
CCCC	$X_m(0)=X'_m(0)=0$	$Y_n(0)=Y'_n(0)=0$	$\sin^2(\alpha x)$	$\sin^2(\beta y)$
	$X_m(a)=X'_m(a)=0$	$Y_n(b)=Y'_n(b)=0$		
CCFF	$X''_m(0)=X'''_m(0)=0$	$Y_n(0)=Y'_n(0)=0$	$\cos^2(\alpha x)\left[\sin^2(\alpha x)+1\right]$	$\sin^2(\beta y)$
	$X''_m(a)=X'''_m(a)=0$	$Y_n(b)=Y'_n(b)=0$		

Table 2 Comparison of the present model for free vibrations of nanocomposite plate

(m, n)	Model	Pure Epoxy	UD	FG-O	FG-X	FG-A
1,1	(Song *et al*. 2017)	0.0584	0.1216	0.1020	0.1378	0.1118
	(Arefi *et al.* 2018)	0.0584	0.1216	0.1023	0.1365	0.1118
	Present	0.05843	0.12158	0.10230	0.13662	0.11178
2,1	(Song *et al.* 2017)	0.1391	0.2895	0.2456	0.3249	0.2673
	(Arefi *et al.* 2018)	0.1391	0.2896	0.2471	0.3183	0.2671
	Present	0.13914	0.28954	0.24698	0.31885	0.26713
2,2	(Song *et al.* 2017)	0.2132	0.4436	0.3796	0.4939	0.4110
	(Arefi *et al.* 2018)	0.2133	0.4438	0.3830	0.4798	0.4107
	Present	0.21321	0.44369	0.38279	0.48090	0.41071
3,1	(Song *et al.* 2017)	0.2595	0.5400	0.4645	0.5984	0.5013
	(Arefi *et al*. 2018)	0.2597	0.5403	0.4694	0.5787	0.5009
	Present	0.25956	0.54018	0.46909	0.58030	0.50030
3,2	(Song *et al*. 2017)	0.3251	0.6767	0.5860	0.7454	0.6299
	(Arefi *et al*. 2018)	0.3254	0.6773	0.5934	0.7168	0.6294
	Present	0.32530	0.67703	0.59304	0.71903	0.62921
3,3	(Song *et al*. 2017)	0.4261	0.8869	0.7755	0.9690	0.8287
	(Arefi *et al.* 2018)	0.4267	0.8881	0.7877	0.9251	0.8282
	Present	0.42651	0.88772	0.78701	0.92836	0.82820

Table 3 Comparison of non-dimensional natural frequency $\bar{\omega}=\omega h\sqrt{\rho_c/G_c}$ of based SUS304/Si_3N_4 FG plate for different nonlocal parameters and boundary conditions (n=5)

a/h	μ	SSSS		CCCC	
		RSDT[a]	Present	RSDT[a]	present
10	0	0.0441	0.04412	0.0758	0.07936
	1	0.0403	0.04032	0.0682	0.07051
	2	0.0374	0.03736	0.0624	0.06408
	4	0.0330	0.03298	0.0542	0.05520
20	0	0.0113	0.01133	0.0207	0.02109
	1	0.0103	0.01036	0.0186	0.01876
	2	0.0096	0.00960	0.0170	0.01701
	4	0.0085	0.00847	0.0147	0.01471

[a]: Ref. (Natarajan *et al.* 2012)

Table 4 Comparison of the present approach for free vibrations ($\hat{\omega} = \omega h\sqrt{\rho_m / E_m}$) of mounted Al/Al2O3 plate

K_W	K_P	a/h	Method	n				
				0	0.5	1	2	5
100	0	5	TSDT[a]	0.4273	0.3758	0.3476	0.3219	0.2999
			Quasi-3D[b]	0.4284	0.3734	0.3431	0.3159	0.2950
			Present	0.42689	0.36969	0.33704	0.30831	0.28910
		20	TSDT[a]	0.0298	0.0258	0.0238	0.0221	0.0210
			Quasi-3D[b]	0.0298	0.0257	0.0236	0.0218	0.0208
			Present	0.02977	0.02554	0.02325	0.02139	0.02044
	100	5	TSDT[a]	0.6162	0.6026	0.5978	0.5970	0.5993
			Quasi-3D[b]	0.6137	0.5940	0.5856	0.5815	0.5843
			Present	0.61562	0.59405	0.58313	0.57691	0.58075
		20	TSDT[a]	0.0411	0.0395	0.0388	0.0386	0.0388
			Quasi-3D[b]	0.0411	0.0393	0.0386	0.0383	0.0385
			Present	0.04106	0.03921	0.03841	0.03804	0.03834

[a]: Ref. (Baferani *et al*. 2011), [b]: Ref. (Shahsavari *et al.* 2018)

To investigate the size-dependent behavior of nanostructure systems, the stiffness-softening mechanism of nanostructures (via Eringen nonlocal model) on the first natural frequency of FG-PC nanoplates reinforced with GNPs for the fixed FG-O pattern are analyzed with respect to the total number of layers of GNPs for different boundary conditions. The results are demonstrated in Fig. 3. It can be seen that for vibration problem, there is a decrement in natural frequency with increase in nonlocal parameter for all boundary conditions. Another important result may be that the reinforced structures made of GNPs is more resistance to higher natural frequency with the increasing number of layers. Furthermore, the effect of the total number of layers from N_L=2 to N_L=5 is more than that from N_L=10 to N_L=20.

Fig. 4 is plotted to show the effect of nonlocality effect on the natural frequency of SSSS FG-PC nanoplates with respect to the GNPs distributions patterns. As a general trend it can be concluded that the nonlocality effect is independent of reinforcement patterns, and the vibration response will always reduce by increasing the nonlocal parameter. Further, it can be seen that the UD pattern and FG-A pattern has almost the same results for SSSS boundary conditions. Furthermore, as FG-PC plate reinforced with GPLs, the greatest natural frequencies of the nanoplate reinforced with GNPs is obtained for the nanoplate with FG-X reinforcement pattern followed by UD, FG-A, and FG-O, respectively.

As a benchmark result, the first natural frequency of square FG-PC nanoplate has been reported in Table 5 for different values of weight fraction of GNP, boundary conditions, reinforcement patterns, and nonlocal parameters. In a similar way with plates, the natural frequency of nanoplates increases with increment in the weight fraction of GNP. Likewise, the plate, which is revealed to have the greatest natural frequencies of the FG-PC nanoplate reinforced with GNPs, is considered for the nanoplate with CCFF boundary conditions followed by CCCC, CSCS, and SSSS, respectively.

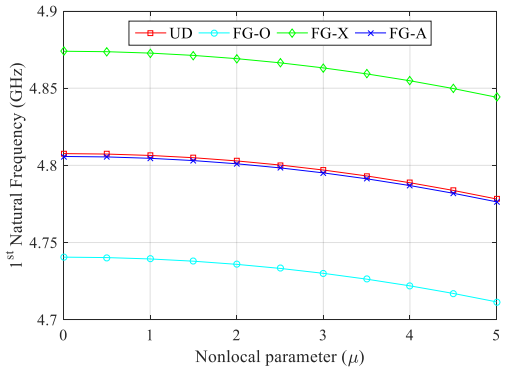

Fig. 4 Influences of nonlocality on the 1st natural frequency (in GHz) of SSSS FG polymer composite nanoplates reinforced with GNPs for each pattern

The impact of the geometry and size of GNPs is investigated vs length-to-thickness ratio (l_{GNP}/h_{GNP}) and the length-to-width ratio (l_{GNP}/w_{GNP}) on the first natural frequency of GNPs reinforced nanoplates with respect to different GNP distribution patterns. Note that the length of GNP l_{GNP} is kept constant. Natural frequency increases as the l_{GNP}/h_{GNP} ratio increases. This demonstrates that GNPs with fewer layers are more effective in growing the frequency of the nanoplate (see Fig. 5). Further, the GNPs reinforced polymer nanocomposite with square GNPs (l_{GNP}/w_{GNP}=1) is seen to have a bigger frequency than its counterpart with rectangular GNPs (l_{GNP}/w_{GNP}=2).

The influences of two-parameter elastic foundation on the first natural frequency have been presented in Table 6 with respect to the different nonlocal parameters, boundary conditions, and GNPs reinforcement patterns. From this table, it is observable that increasing of linear and shear coefficients of Winkler-Pasternak foundation leads to the increasing natural frequency, and this conclusion is independent of boundary conditions, nonlocality, and GNPs reinforcement patterns. Moreover, the impact of the shear layer of the elastic foundation is more than linear layer once. Therefore, it is very important to regard the shear

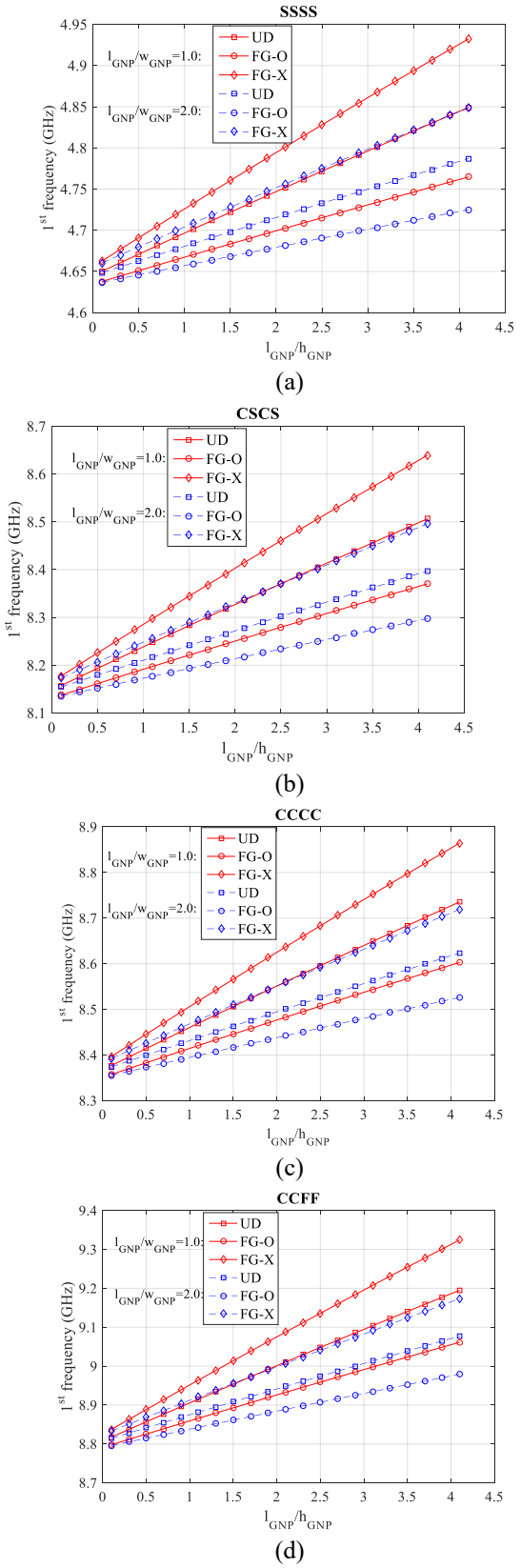

Fig. 5 The GNPs geometry and size impacts on the natural frequency (in GHz), (μ=1 nm, g^*_{GNP}=1 %, l_{GNP}=3 nm).

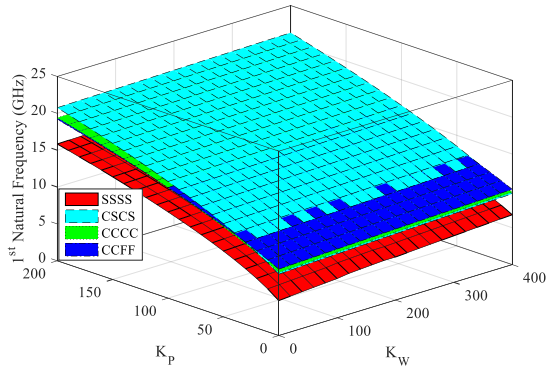

Fig. 6 Winkler-Pasternak foundation effects on the 1st natural frequency different boundary conditions, and a fixed FG-O Pattern, (μ=1 nm, g^*_{GNP}=1 %).

layer of an elastic foundation in the analysis of FG-PC nanoplates reinforced with GNPs. To better understanding of this issue, the effect of Winkler-Pasternak foundation on the first natural frequency of GNPs reinforced nanoplates for fixed FG-O pattern is illustrated in Fig. 6. It can be seen that for the analysis of nanostructures, considering the role of size effects and boundary conditions are important to perform and accurate design.

6. Conclusions

This study investigated the effects of boundary conditions on the dynamic characteristics of GNPs reinforced nanocomposite nanoplates considering the size-dependent effect. Using the rule of mixture in conjunction with the Halpin-Tsai micromechanical modeling, the effective properties of the material with uniform and three different non-uniform patterns of GNPs distributions were achieved. Employing Hamilton's principle, governing equations of motion and boundary conditions were obtained Eringen nonlocal differential model in conjunction with a four unknown refined plate theory. Galerkin method was utilized to solve the size-dependent natural frequency of the nanoplates reinforced with GNPs for different boundary conditions. It was found that the natural frequency increases with an increment in Winkler-Pasternak foundation parameters and a decrement in the nonlocal parameter. It can be emphasized that stiffer structures have greater natural frequencies and can reduce the impact of reinforcement pattern on the results. Moreover, it was reported that the effect of weight fraction of GNPs on the vibration characteristics of GNPs reinforced nanoplates is more considerable for a bigger value of weight fraction of GNPs. Further, an addition of a number of layers of GNPs can decrease the natural frequencies of the GNPs reinforced nanoplates. It was also revealed that the greatest natural frequencies of the square FG-PC macro/nano-plates reinforced with GPLs/GNPs is obtained for the plate with CCFF (FG-X) boundary conditions (distribution patterns of GNPs or GPLs) followed by CCCC (UD), CSCS (FG-A), and SSSS (FG-O), respectively.

Table 5 Natural frequencies (in GHz) of the nanoplate for different weight fractions g^*_{GNP}, patterns, nonlocal parameters, and boundary conditions, (N_L=10)

		UD					FG-O					FG-X				
g^*_{GNP} (%)	B.C	μ=0	μ=1	μ=2	μ=3	μ=4	μ=0	μ=1	μ=2	μ=3	μ=4	μ=0	μ=1	μ=2	μ=3	μ=4
0.2	SSSS	4.6574	4.6562	4.6528	4.6471	4.6391	4.4638	4.6426	4.6392	4.6335	4.6256	4.6709	4.6698	4.6663	4.6606	4.6526
	CSCS	8.1708	8.1676	8.1579	8.1418	8.1194	8.1491	8.1459	8.1362	8.1201	8.0978	8.1925	8.1892	8.1795	8.1634	8.1409
	CCCC	8.3900	8.3872	8.3788	8.3649	8.3455	8.3689	8.3661	8.3578	8.3439	8.3245	8.4110	8.4082	8.3998	8.3859	8.3664
	CCFF	8.8310	8.8282	8.8198	8.8058	8.7863	8.8098	8.8070	8.7986	8.7847	8.7653	8.8521	8.8493	8.8408	8.8268	8.8073
0.4	SSSS	4.6952	4.6940	4.6905	4.6848	4.6767	4.6681	4.6669	4.6635	4.6578	4.6498	4.7221	4.7209	4.7174	4.7116	4.7036
	CSCS	8.2372	8.2340	8.2242	8.2080	8.1854	8.1939	8.1906	8.1809	8.1647	8.1423	8.2803	8.2770	8.2672	8.2508	8.2282
	CCCC	8.4583	8.4555	8.4470	8.4330	8.4134	8.4162	8.4133	8.4049	8.3909	8.3715	8.5000	8.4972	8.4887	8.4746	8.4549
	CCFF	8.9029	8.9001	8.8916	8.8775	8.8579	8.8606	8.8578	8.8493	8.8353	8.8158	8.9448	8.9419	8.9333	8.9192	8.8995
0.6	SSSS	4.7328	4.7316	4.7281	4.7223	4.7142	4.6923	4.6912	4.6877	4.6819	4.6739	4.7730	4.7718	4.7683	4.7624	4.7543
	CSCS	8.3034	8.3001	8.2902	8.2739	8.2511	8.2384	8.2352	8.2254	8.2092	8.1866	8.3685	8.3642	8.3543	8.3378	8.3149
	CCCC	8.5263	8.5234	8.5149	8.5007	8.4810	8.4632	8.4603	8.4519	8.4378	8.4183	8.5884	8.5856	8.5770	8.5627	8.5429
	CCFF	8.9745	8.9717	8.9631	8.9489	8.9291	8.9111	8.9083	8.8998	8.8857	8.8660	9.0368	9.0340	9.0253	9.0110	8.9911
0.8	SSSS	4.7703	4.7691	4.7656	4.7597	4.7516	4.7165	4.7153	4.7118	4.7060	4.6980	4.8236	4.8224	4.8188	4.8129	4.8047
	CSCS	8.3692	8.3659	8.3560	8.3395	8.3166	8.2829	8.2796	8.2698	8.2534	8.2308	8.4543	8.4509	8.4409	8.4243	8.4011
	CCCC	8.5940	8.5911	8.5825	8.5682	8.5484	8.5100	8.5072	8.4986	8.4845	8.4648	8.6764	8.6735	4.6648	8.6504	8.6303
	CCFF	9.0458	9.0430	9.0343	9.0200	9.0001	8.9614	8.9586	8.9500	8.9358	8.9161	9.1284	9.1255	9.1168	9.1023	9.0822
1	SSSS	4.8076	4.8064	4.8029	4.7970	4.7888	4.7406	4.7394	4.7359	4.7301	4.7219	4.8739	4.8727	4.8691	4.8631	4.8548
	CSCS	8.4349	8.4315	8.4215	8.4049	8.3818	8.3272	8.3239	8.3140	8.2976	8.2747	8.5406	8.5372	8.5271	8.5102	8.4868
	CCCC	8.6614	8.6585	8.6499	8.6355	8.6155	8.5567	8.5538	8.5452	8.5310	8.5112	8.7638	8.7608	8.7521	8.7375	8.7173
	CCFF	9.1169	9.114	9.1053	9.0909	9.0708	9.0115	9.0087	9.0001	8.9858	8.9659	9.2194	9.2165	9.2077	9.1931	9.1728

Table 6 Natural frequencies (in GHz) of the nanooplate for different elastic foundation parameters, patterns, nonlocal parameter, and boundary conditions, (N_L=10).

		UD					FG-O					FG-X				
(K_W, K_P)	B.C	μ=0	μ=1	μ=2	μ=3	μ=4	μ=0	μ=1	μ=2	μ=3	μ=4	μ=0	μ=1	μ=2	μ=3	μ=4
(100,0)	SSSS	5.3782	5.3771	5.3739	5.3687	5.3613	5.3782	5.3771	5.3739	5.3687	5.3613	5.4376	5.4365	5.4333	5.4279	5.4204
	CSCS	8.7706	8.7673	8.7577	8.7417	8.7195	8.7706	8.7673	8.7577	8.7417	8.7195	8.8724	8.8691	8.8593	8.8431	8.8206
	CCCC	8.9901	8.9873	8.9789	8.9651	8.9458	8.9901	8.9873	8.9789	8.9651	8.9458	9.0888	9.0860	9.0775	9.0635	9.0440
	CCFF	9.4302	9.4274	9.4190	9.4050	9.3855	9.4302	9.4274	9.4190	9.4050	9.3855	9.5294	9.5266	9.5181	9.5039	9.4843
(100,100)	SSSS	11.9847	11.9795	11.9639	11.9380	11.9019	11.9575	11.9523	11.9368	11.9109	11.8747	12.0119	12.0067	11.9911	11.9652	11.9291
	CSCS	16.1029	16.0910	16.0559	15.9955	15.9125	16.0454	16.0334	15.9976	15.9380	15.8550	16.1600	16.1480	16.1121	16.0525	15.9695
	CCCC	15.2807	15.2692	15.2345	15.1770	15.0966	15.2204	15.2088	15.1742	15.1166	15.0362	15.3402	15.3286	15.2940	15.2365	15.1562
	CCFF	15.2928	15.2806	15.2440	15.1830	15.0979	15.2291	15.2168	15.1801	15.1191	15.0339	15.3554	15.3432	15.3066	15.2456	15.1606
(200,100)	SSSS	12.2247	12.2196	12.2044	12.1790	12.1436	12.1981	12.1930	12.1777	12.1523	12.1169	12.2514	12.2463	12.2311	12.2057	12.1702
	CSCS	16.2812	16.2694	16.2339	16.1750	16.0929	16.2243	16.2124	16.1770	16.1181	16.0360	16.3377	16.3258	16.2903	16.2314	16.1493
	CCCC	15.4694	15.4579	15.4237	15.3669	15.2875	15.4097	15.3983	15.3641	15.3072	15.2278	15.5282	15.5167	15.4826	15.4257	15.3464
	CCFF	15.4816	15.4696	15.4334	15.3731	15.2890	15.4186	15.4065	15.3703	15.3100	15.2258	15.5435	15.5314	15.4952	15.4350	15.3510
(200,200)	SSSS	16.2523	16.2450	16.2231	16.1866	16.1358	16.2319	16.2246	16.2027	16.1663	16.1154	16.2727	16.2654	16.2435	16.2070	16.1561
	CSCS	21.1521	21.1352	21.0845	21.0005	20.8833	21.1072	21.0904	21.0397	20.9557	20.8385	21.1966	21.1797	21.1291	21.0450	20.9278
	CCCC	19.7978	19.7812	19.7316	19.6490	19.5337	19.7503	19.7337	19.6841	19.6014	19.4861	19.8447	19.8281	19.7785	19.6959	19.5807
	CCFF	19.6113	19.5936	19.5404	19.4520	19.3285	19.5606	19.5429	19.4897	19.4013	19.2776	19.6611	19.6434	19.5903	19.5019	19.3785

“”

References

Abdelaziz, H.H., Meziane, M.A.A., Bousahla, A.A., Tounsi, A., Mahmoud, S. and Alwabli, A.S. (2017), “An efficient hyperbolic shear deformation theory for bending, buckling and free vibration of FGM sandwich plates with various boundary conditions”, *Steel Compos. Struct.*, **25**(6), 693-704. https://doi.org/10.12989/scs.2017.25.6.693.

Arefi, M., Bidgoli, E.M.R., Dimitri, R. and Tornabene, F. (2018), “Free vibrations of functionally graded polymer composite nanoplates reinforced with graphene nanoplatelets”, *Aerosp. Sci. Technol.*, **81** 108-117. https://doi.org/10.1016/j.ast.2018.07.036.

Baferani, A.H., Saidi, A. and Ehteshami, H. (2011), “Accurate solution for free vibration analysis of functionally graded thick rectangular plates resting on elastic foundation”, *Compos. Struct.*, **93**(7), 1842-1853. https://doi.org/10.1016/j.compstruct.2011.01.020.

Barati, M.R. and Zenkour, A.M. (2018), “Electro-thermoelastic vibration of plates made of porous functionally graded piezoelectric materials under various boundary conditions”, *J. Vib. Control*, **24**(10), 1910-1926. https://doi.org/10.1177/1077546316672788`

Benahmed, A., Fahsi, B., Benzair, A., Zidour, M., Bourada, F. and Tounsi, A. (2019), “Critical buckling of functionally graded nanoscale beam with porosities using nonlocal higher-order

shear deformation", *Struct. Eng. Mech*., **69**(4), 457-466. https://doi.org/10.12989/sem.2019.69.4.457.

Bisen, H.B., Hirwani, C.K., Satankar, R.K., Panda, S.K., Mehar, K. and Patel, B. (2018), "Numerical study of frequency and deflection responses of natural fiber (Luffa) reinforced polymer composite and experimental validation", *J. Natural Fibers*, https://doi.org/10.1080/15440478.2018.1503129.

Bouafia, K., Kaci, A., Houari, M.S.A., Benzair, A. and Tounsi, A. (2017), "A nonlocal quasi-3D theory for bending and free flexural vibration behaviors of functionally graded nanobeams", *Smart Struct. Syst.*, **19**(2), 115-126. https://doi.org/10.12989/sss.2017.19.2.115.

Bounouara, F., Benrahou, K.H., Belkorissat, I. and Tounsi, A. (2016), "A nonlocal zeroth-order shear deformation theory for free vibration of functionally graded nanoscale plates resting on elastic foundation", *Steel Compos. Struct*., **20**(2), 227-249. https://doi.org/10.12989/scs.2016.20.2.227.

Canales, F. and Mantari, J. (2018), "Free vibration of thick isotropic and laminated beams with arbitrary boundary conditions via unified formulation and Ritz method", *Appl. Math. Model*., **61**, 693-708. https://doi.org/10.1016/j.apm.2018.05.005.

Chen, D., Yang, J. and Kitipornchai, S. (2017), "Nonlinear vibration and postbuckling of functionally graded graphene reinforced porous nanocomposite beams", *Compos. Sci. Technol*., **142**, 235-245. https://doi.org/10.1016/j.compscitech.2017.02.008.

Dash, S., Mehar, K., Sharma, N., Mahapatra, T.R. and Panda, S.K. (2018), "Modal analysis of FG sandwich doubly curved shell structure", *Struct. Eng. Mech*., **68**(6), 721-733. https://doi.org/10.12989/sem.2018.68.6.721.

Dash, S., Mehar, K., Sharma, N., Mahapatra, T.R. and Panda, S.K. (2019), "Finite element solution of stress and flexural strength of functionally graded doubly curved sandwich shell panel", *Earthq. Struct.*, **16**(1), 55-67. https://doi.org/10.12989/eas.2019.16.1.055.

Eringen, A.C. (1983), "On differential equations of nonlocal elasticity and solutions of screw dislocation and surface waves", *J. Appl. Phys*., **54**(9), 4703-4710. https://doi.org/10.1063/1.332803.

Eyvazian, A., Hamouda, A.M., Tarlochan, F., Mohsenizadeh, S. and Dastjerdi, A.A. (2019), "Damping and vibration response of viscoelastic smart sandwich plate reinforced with non-uniform graphene platelet with magnetorheological fluid core", *Steel Compos. Struct*., **33**(6), 891-906. https://doi.org/10.12989/scs.2019.33.6.891.

Eyvazian, A., Shahsavari, D. and Karami, B. (2020), "On the dynamic of graphene reinforced nanocomposite cylindrical shells subjected to a moving harmonic load", *Int. J. Eng. Sci.*, 154 103339. https://doi.org/10.1016/j.ijengsci.2020.103339.

Farajpour, A., Ghayesh, M.H. and Farokhi, H. (2018), "A review on the mechanics of nanostructures", *Int. J. Eng. Sci*., **133**, 231-263. https://doi.org/10.1016/j.ijengsci.2018.09.006.

Farajpour, A., Ghayesh, M.H. and Farokhi, H. (2019), "Frequency response of initially deflected nanotubes conveying fluid via a nonlinear NSGT model", *Struct. Eng. Mech*., **72**(1), 71-81. https://doi.org/10.12989/sem.2019.72.1.071.

Farajpour, A., Ghayesh, M.H. and Farokhi, H. (2019), "Nonlocal nonlinear mechanics of imperfect carbon nanotubes", *Int. J. Eng. Sci*., **142**, 201-215. https://doi.org/10.1016/j.ijengsci.2019.03.003.

Farzam, A. and Hassani, B. (2018), "Thermal and mechanical buckling analysis of FG carbon nanotube reinforced composite plates using modified couple stress theory and isogeometric approach", *Compos. Struct*., **206** 774-790. https://doi.org/10.1016/j.compstruct.2018.08.030.

Fattahi, A., Safaei, B. and Moaddab, E. (2019), "The application of nonlocal elasticity to determine vibrational behavior of FG nanoplates", *Steel Compos. Struct*., **32**(2), 281-292. https://doi.org/10.12989/scs.2019.32.2.281.

Ghayesh, M.H. (2014), "Nonlinear size-dependent behaviour of single-walled carbon nanotubes", *Appl. Physics A*, **117**(3), 1393-1399. https://doi.org/10.1007/s00339-014-8561-6.

Ghayesh, M.H. (2018), "Dynamics of functionally graded viscoelastic microbeams", *Int. J. Eng. Sci*., **124**, 115-131. https://doi.org/10.1016/j.ijengsci.2017.11.004.

Ghayesh, M.H. and Farajpour, A. (2019), "A review on the mechanics of functionally graded nanoscale and microscale structures", *Int. J. Eng. Sci*., **137**, 8-36. https://doi.org/10.1016/j.ijengsci.2018.12.001.

Ghayesh, M.H., Farokhi, H. and Alici, G. (2016), "Size-dependent performance of microgyroscopes", *Int. J. Eng. Sci*., **100**, 99-111. https://doi.org/10.1016/j.ijengsci.2015.11.003.

Gholami, R. and Ansari, R. (2018), "On the Nonlinear Vibrations of Polymer Nanocomposite Rectangular Plates Reinforced by Graphene Nanoplatelets: A Unified Higher-Order Shear Deformable Model", *Iranian J. Sci. Technol. T. Mech. Eng*., 1-18. https://doi.org/10.1007/s40997-018-0182-9.

Gholipour, A. and Ghayesh, M.H. (2020), "Nonlinear coupled mechanics of functionally graded nanobeams", *Int. J. Eng. Sci.*, **150**, 103221. https://doi.org/10.1016/j.ijengsci.2020.103221.

Hebali, H., Bakora, A., Tounsi, A. and Kaci, A. (2016), "A novel four variable refined plate theory for bending, buckling, and vibration of functionally graded plates", *Steel Compos. Struct*., **22**(3), 473-495. https://doi.org/10.12989/scs.2016.22.3.473.

Houari, M.S.A., Bessaim, A., Bernard, F., Tounsi, A. and Mahmoud, S. (2018), "Buckling analysis of new quasi-3D FG nanobeams based on nonlocal strain gradient elasticity theory and variable length scale parameter", *Steel Compos. Struct*., **28**(1), 13-24. https://doi.org/10.12989/scs.2018.28.1.013.

Imran, M., Khan, R. and Badshah, S. (2018), "Finite Element Analysis to Investigate the Influence of Delamination Size, Stacking Sequence and Boundary Conditions on the Vibration Behavior of Composite Plate", *Iranian J. Mater. Sci. Eng*., **15**(3), 11-21. https://doi.org/10.22068/ijmse.16.1.11.

Karami, B., Gheisari, P., Nazemosadat, S.M.R., Akbari, P., Shahsavari, D. and Naghizadeh, M. (2020), "Elastic wave characteristics of graphene nanoplatelets reinforced composite nanoplates", *Struct. Eng. Mech*., **74**(6), 809-819. https://doi.org/10.12989/sem.2020.74.6.809.

Karami, B. and Janghorban, M. (2020), "On the mechanics of functionally graded nanoshells", *Int. J. Eng. Sci*., **153**, 103309. https://doi.org/10.1016/j.ijengsci.2020.103309.

Karami, B., Janghorban, M., Shahsavari, D., Dimitri, R. and Tornabene, F. (2019), "Nonlocal buckling analysis of composite curved beams reinforced with functionally graded carbon nanotubes", *Molecules*, **24**(15), 2750. https://doi.org/10.3390/molecules24152750.

Karami, B. and Shahsavari, D. (2020), "On the forced resonant vibration analysis of functionally graded polymer composite doubly-curved nanoshells reinforced with graphene-nanoplatelets", *Comput. Method. Appl. M*., **359**, 112767. https://doi.org/10.1016/j.cma.2019.112767.

Karami, B., Shahsavari, D. and Janghorban, M. (2018), "A Comprehensive Analytical Study on Functionally Graded Carbon Nanotube-Reinforced Composite Plates", *Aerosp. Sci. Technol*., https://doi.org/10.1016/j.ast.2018.10.001.

Karami, B., Shahsavari, D., Janghorban, M. and Li, L. (2019), "Elastic guided waves in fully-clamped functionally graded carbon nanotube-reinforced composite plates", *Mater. Res. Express*, **6**(9), 0950a0959. https://doi.org/10.1088/2053-1591/ab3474

Karami, B., Shahsavari, D., Janghorban, M. and Li, L. (2020), "Free vibration analysis of FG nanoplate with poriferous

imperfection in hygrothermal environment", *Struct. Eng. Mech*., **73**(2), 191-207. https://doi.org/10.12989/sem.2020.73.2.191.

Karami, B., Shahsavari, D., Janghorban, M. and Tounsi, A. (2019), "Resonance behavior of functionally graded polymer composite nanoplates reinforced with graphene nanoplatelets", *Int. J. Mech. Sci*., **156**, 94-105. https://doi.org/10.1016/j.ijmecsci.2019.03.036.

Karami, B., Shahsavari, D., Nazemosadat, S.M.R., Li, L. and Ebrahimi, A. (2018), "Thermal buckling of smart porous functionally graded nanobeam rested on Kerr foundation", *Steel Compos. Struct*., **29**(3), 349-362. https://doi.org/10.12989/scs.2018.29.3.349.

Khan, S.U., Li, C.Y., Siddiqui, N.A. and Kim, J.-K. (2011), "Vibration damping characteristics of carbon fiber-reinforced composites containing multi-walled carbon nanotubes", *Compos. Sci. Technol*., **71**(12), 1486-1494. https://doi.org/10.1016/j.compscitech.2011.03.022.

Kim, K., Choe, K., Kim, S. and Wang, Q. (2018), "A modeling method for vibration analysis of cracked laminated composite beam of uniform rectangular cross-section with arbitrary boundary condition", *Compos. Struct*., https://doi.org/10.1016/j.compstruct.2018.10.006.

Kitipornchai, S., Chen, D. and Yang, J. (2017), "Free vibration and elastic buckling of functionally graded porous beams reinforced by graphene platelets", *Mater. Design*. **116** 656-665. https://doi.org/10.1016/j.matdes.2016.12.061.

Kumar, R., Dey, T. and Panda, S.K. (2019), "Instability and vibration analyses of FG cylindrical panels under parabolic axial compressions", *Steel Compos. Struct*., **31**(2), 187-199. https://doi.org/10.12989/scs.2019.31.2.187.

Mehar, K. and Kumar Panda, S. (2018), "Thermal free vibration behavior of FG-CNT reinforced sandwich curved panel using finite element method", *Polymer Compos*., **39**(8), 2751-2764. https://doi.org/10.1002/pc.24266.

Mehar, K., Mahapatra, T.R., Panda, S.K., Katariya, P.V. and Tompe, U.K. (2018), "Finite-element solution to nonlocal elasticity and scale effect on frequency behavior of shear deformable nanoplate structure", *J. Eng. Mech*., **144**(9), 04018094. https://doi.org/10.1061/(ASCE)EM.1943-7889.0001519.

Mehar, K., Mishra, P. and Panda, S. (2020), "Numerical investigation of thermal frequency responses of graded hybrid smart nanocomposite (CNT-SMA-Epoxy) structure", *Mech. Adv. Mater. Struct*., 1-13. https://doi.org/10.1080/15376494.2020.1725193.

Mehar, K. and Panda, S. (2015). "Free vibration and bending behaviour of CNT reinforced composite plate using different shear deformation theory", *Proceedings of the 5th National Conference on Processing and Characterization of Materials*, https://doi:10.1088/1757-899X/115/1/012014.

Mehar, K. and Panda, S.K. (2016), "Geometrical nonlinear free vibration analysis of FG-CNT reinforced composite flat panel under uniform thermal field", *Compos. Struct*., **143**, 336-346. https://doi.org/10.1016/j.compstruct.2016.02.038.

Mehar, K. and Panda, S.K. (2018). "Dynamic response of functionally graded carbon nanotube reinforced sandwich plate", *Proceedings of the IOP Conference Series: Materials Science and Engineering*, https://doi.org/10.1088/1757-899X/338/1/012017.

Mehar, K. and Panda, S.K. (2019), "Multiscale modeling approach for thermal buckling analysis of nanocomposite curved structure", *Adv. Nano Res*., **7**(3), 181. http://dx.doi.org/10.12989/anr.2019.7.3.181.

Mehar, K. and Panda, S.K. (2019), "Theoretical deflection analysis of multi-walled carbon nanotube reinforced sandwich panel and experimental verification", *Compos. Part B: Eng*., **167**, 317-328. https://doi.org/10.1016/j.compositesb.2018.12.058.

Mehar, K. and Panda, S.K. (2020), "Nonlinear deformation and stress responses of a graded carbon nanotube sandwich plate structure under thermoelastic loading", *Acta Mechanica*, **231**(3), 1105-1123. https://doi.org/10.1007/s00707-019-02579-5.

Mehar, K., Panda, S.K., Bui, T.Q. and Mahapatra, T.R. (2017), "Nonlinear thermoelastic frequency analysis of functionally graded CNT-reinforced single/doubly curved shallow shell panels by FEM", J. Thermal Stresses, 40(7), 899-916. https://doi.org/10.1080/01495739.2017.1318689.

Mehar, K., Panda, S.K., Dehengia, A. and Kar, V.R. (2016), "Vibration analysis of functionally graded carbon nanotube reinforced composite plate in thermal environment", *J. Sandw. Struct. Mater*., **18**(2), 151-173. https://doi.org/10.1177/1099636215613324.

Mehar, K., Panda, S.K., Devarajan, Y. and Choubey, G. (2019), "Numerical buckling analysis of graded CNT-reinforced composite sandwich shell structure under thermal loading", *Compos. Struct*., **216**, 406-414. https://doi.org/10.1016/j.compstruct.2019.03.002.

Mehar, K., Panda, S.K. and Mahapatra, T.R. (2017), "Theoretical and experimental investigation of vibration characteristic of carbon nanotube reinforced polymer composite structure", *Int. J. Mech. Sci.*, **133**, 319-329. https://doi.org/10.1016/j.ijmecsci.2017.08.057.

Mehar, K., Panda, S.K. and Mahapatra, T.R. (2017), "Thermoelastic nonlinear frequency analysis of CNT reinforced functionally graded sandwich structure", *Eur. J. Mech.-A/Solids*, **65**, 384-396. https://doi.org/10.1016/j.euromechsol.2017.05.005.

Mehar, K., Panda, S.K. and Mahapatra, T.R. (2018), "Nonlinear frequency responses of functionally graded carbon nanotube-reinforced sandwich curved panel under uniform temperature field", *Int. J. Appl. Mech*., **10**(3), 1850028. https://doi.org/10.1142/S175882511850028X.

Mehar, K., Panda, S.K. and Mahapatra, T.R. (2019), "Large deformation bending responses of nanotube-reinforced polymer composite panel structure: Numerical and experimental analyses", *Proceedings of the Institution of Mechanical Engineers, Part G: Journal of Aerospace Engineering*, **233**(5), 1695-1704. https://doi.org/10.1177/0954410018761192

Mehar, K., Panda, S.K. and Patle, B.K. (2017), "Thermoelastic vibration and flexural behavior of FG-CNT reinforced composite curved panel", *Int. J. Appl. Mech*., **9**(4), 1750046. https://doi.org/10.1142/S1758825117500466.

Mehar, K., Panda, S.K. and Sharma, N. (2020), "Numerical investigation and experimental verification of thermal frequency of carbon nanotube-reinforced sandwich structure", *Eng. Struct.*, **211**, 110444. https://doi.org/10.1016/j.engstruct.2020.110444.

Mehar, K. and Panda, S.K. (2016), "Geometrical nonlinear free vibration analysis of FG-CNT reinforced composite flat panel under uniform thermal field", *Compos. Struct*., **143**, 336-346. https://doi.org/10.1016/j.compstruct.2016.02.038.

Meziane, M.A.A., Abdelaziz, H.H. and Tounsi, A. (2014), "An efficient and simple refined theory for buckling and free vibration of exponentially graded sandwich plates under various boundary conditions", *J. Sandw. Struct. Mater.*, **16**(3), 293-318. https://doi.org/10.1177/1099636214526852.

Motezaker, M. and Eyvazian, A. (2020), "Post-buckling analysis of Mindlin Cut out-plate reinforced by FG-CNTs", *Steel Compos. Struct*., **34**(2), 289-297. https://doi.org/10.12989/scs.2020.34.2.289.

Natarajan, S., Chakraborty, S., Thangavel, M., Bordas, S. and Rabczuk, T. (2012), "Size-dependent free flexural vibration behavior of functionally graded nanoplates", *Comput. Mater. Sci*., **65**, 74-80. https://doi.org/10.1016/j.commatsci.2012.06.031.

Panda, S.K. and Singh, B. (2013), "Nonlinear finite element analysis of thermal post-buckling vibration of laminated

composite shell panel embedded with SMA fibre", *Aerosp. Sci. Technol.*, **29**(1), 47-57. https://doi.org/10.1016/j.ast.2013.01.007.

Phung-Van, P., Lieu, Q.X., Nguyen-Xuan, H. and Wahab, M.A. (2017), "Size-dependent isogeometric analysis of functionally graded carbon nanotube-reinforced composite nanoplates", *Compos. Struct*., **166**, 120-135. https://doi.org/10.1016/j.compstruct.2017.01.049.

Quaresimin, M., Schulte, K., Zappalorto, M. and Chandrasekaran, S. (2016), "Toughening mechanisms in polymer nanocomposites: From experiments to modelling", *Compos. Sci. Technol*., **123**, 187-204. https://doi.org/10.1016/j.compscitech.2015.11.027.

Radić, N. and Jeremić, D. (2017), "A comprehensive study on vibration and buckling of orthotropic double-layered graphene sheets under hygrothermal loading with different boundary conditions", *Compos. Part B: Eng*., **128**, 182-199. https://doi.org/10.1016/j.compositesb.2017.07.019.

Rafiee, M.A., Rafiee, J., Wang, Z., Song, H., Yu, Z.Z. and Koratkar, N. (2009), "Enhanced mechanical properties of nanocomposites at low graphene content", *ACS Nano*, **3**(12), 3884-3890. https://doi.org/10.1021/nn9010472.

Sahmani, S., Aghdam, M.M. and Rabczuk, T. (2018), "Nonlinear bending of functionally graded porous micro/nano-beams reinforced with graphene platelets based upon nonlocal strain gradient theory", *Compos. Struct.*, **186**, 68-78. https://doi.org/10.1016/j.compstruct.2017.11.082.

Shahsavari, D., Karami, B. and janghorban, M. (2019), "On buckling analysis of laminated composite plates using a nonlocal refined four-variable model", *Steel Compos. Struct*., **32**(2), 173-187. https://doi.org/10.12989/scs.2019.32.2.173.

Shahsavari, D., Karami, B. and Janghorban, M. (2019), "Size-dependent vibration analysis of laminated composite plates", *Adv. Nano Res*., **7**(5), 337-349. https://doi.org/10.12989/anr.2019.7.5.337.

Shahsavari, D., Karami, B., Janghorban, M. and Li, L. (2017), "Dynamic characteristics of viscoelastic nanoplates under moving load embedded within visco-Pasternak substrate and hygrothermal environment", *Mater. Res. Express*, **4**(8), 085013. https://doi.org/10.1088/2053-1591/aa7d89.

Shahsavari, D., Shahsavari, M., Li, L. and Karami, B. (2018), "A novel quasi-3D hyperbolic theory for free vibration of FG plates with porosities resting on Winkler/Pasternak/Kerr foundation", *Aerosp. Sci. Technol.*, **72**, 134-149. https://doi.org/10.1016/j.ast.2017.11.004.

Singh, V.K., Hirwani, C.K., Panda, S.K., Mahapatra, T.R. and Mehar, K. (2019), "Numerical and experimental nonlinear dynamic response reduction of smart composite curved structure using collocation and non-collocation configuration", *Proceedings of the Institution of Mechanical Engineers, Part C: Journal of Mechanical Engineering Science*, **233**(5), 1601-1619. https://doi.org/10.1177/0954406218774362.

Sobhy, M. (2013), "Buckling and free vibration of exponentially graded sandwich plates resting on elastic foundations under various boundary conditions", *Compos. Struct.*, **99** 76-87. https://doi.org/10.1016/j.compstruct.2012.11.018

Song, M., Kitipornchai, S. and Yang, J. (2017), "Free and forced vibrations of functionally graded polymer composite plates reinforced with graphene nanoplatelets", *Compos. Struct*., **159** 579-588. https://doi.org/10.1016/j.compstruct.2016.09.070.

Song, M., Yang, J. and Kitipornchai, S. (2018), "Bending and buckling analyses of functionally graded polymer composite plates reinforced with graphene nanoplatelets", *Compos. Part B: Eng*., **134**, 106-113. https://doi.org/10.1016/j.compositesb.2017.09.043

Tahouneh, V., Naei, M.H. and Mashhadi, M.M. (2019), "Using IGA and trimming approaches for vibrational analysis of L-shape graphene sheets via nonlocal elasticity theory", *Steel Compos. Struct.*, **33**(5), 717. https://doi.org/10.12989/scs.2019.33.5.717.

Thanh, C.-L., Phung-Van, P., Thai, C.H., Nguyen-Xuan, H. and Wahab, M.A. (2018), "Isogeometric analysis of functionally graded carbon nanotube reinforced composite nanoplates using modified couple stress theory", *Compos. Struct.*, **184**, 633-649. https://doi.org/10.1016/j.compstruct.2017.10.025.

Wang, A., Chen, H., Hao, Y. and Zhang, W. (2018), "Vibration and bending behavior of functionally graded nanocomposite doubly-curved shallow shells reinforced by graphene nanoplatelets", *Results in Physics*, **9**, 550-559. https://doi.org/10.1016/j.rinp.2018.02.062.

Yang, J., Chen, D. and Kitipornchai, S. (2018), "Buckling and free vibration analyses of functionally graded graphene reinforced porous nanocomposite plates based on Chebyshev-Ritz method", *Compos. Struct*., **193**, 281-294. https://doi.org/10.1016/j.compstruct.2018.03.090.

Zhao, J., Choe, K., Xie, F., Wang, A., Shuai, C. and Wang, Q. (2018), "Three-dimensional exact solution for vibration analysis of thick functionally graded porous (FGP) rectangular plates with arbitrary boundary conditions", *Compos. Part B: Eng*., **155**, 369-381. https://doi.org/10.1016/j.compositesb.2018.09.001.

Zhao, Z., Feng, C., Wang, Y. and Yang, J. (2017), "Bending and vibration analysis of functionally graded trapezoidal nanocomposite plates reinforced with graphene nanoplatelets (GPLs)", *Compos. Struct.*, **180,** 799-808. https://doi.org/10.1016/j.compstruct.2017.08.044.

Zhong, R., Wang, Q., Tang, J., Shuai, C. and Liang, Q. (2018), "Vibration characteristics of functionally graded carbon nanotube reinforced composite rectangular plates on Pasternak foundation with arbitrary boundary conditions and internal line supports", *Curved Layered Struct*., **5**(1), 10-34. https://doi.org/10.1515/cls-2018-0002

Zidi, M., Tounsi, A., Houari, M.S.A. and Bég, O.A. (2014), "Bending analysis of FGM plates under hygro-thermo-mechanical loading using a four variable refined plate theory", *Aerosp. Sci. Technol*., **34** 24-34. https://doi.org/10.1016/j.ast.2014.02.001.

CC